Percutaneous Kidney Puncture with Three-dimensional Mixed-reality Hologram Guidance: From Preoperative Planning to Intraoperative Navigation

Percutaneous Kidney Puncture with Three-dimensional Mixed-reality Hologram Guidance: From Preoperative Planning to Intraoperative Navigation

Francesco Porpiglia [a 1],
Enrico Checcucci [a b c 1],
Daniele Amparore [a],
Dario Peretti [a], Federico Piramide [a],
Sabrina De Cillis [a], Alberto Piana [a],
Gabriel Niculescu [a],
Paolo Verri [a],
Matteo Manfredi [a],
Massimiliano Poggio [a],
Ilaria Stura [d],
Giuseppe Migliaretti [d],
Marco Cossu [a 1],
Cristian Fiori [a 1]

[a]Division of Urology, Department Of Oncology, School of Medicine, University of Turin, San Luigi Hospital, Orbassano, Turin, Italy
[b]Department of Surgery, Candiolo Cancer Institute, FPO-IRCCS, Candiolo, Turin, Italy
[c]Uro-technology and Social Media Working Group of the Young Academic Urologists of the European Association of Urology, Arnhem, The Netherlands
[d]Department of Public Health and Pediatric Sciences, School of Medicine, University of Turin, Turin, Italy

Abstract

Background
Despite technical and technological innovations, percutaneous puncture still represents the most challenging step when performing percutaneous nephrolithotomy. This maneuver is characterized by the steepest learning curve and a risk of injuring surrounding organs and kidney damage.

Objective
To evaluate the feasibility of three-dimensional mixed reality (3D MR) holograms in establishing the access point and guiding the needle during percutaneous kidney puncture.

Design, setting, and participants
This prospective study included ten patients who underwent 3D MR endoscopic combined intrarenal surgery (ECIRS) for kidney stones from July 2019 to January 2020. A retrospective series of patients who underwent a standard procedure were selected for matched pair analysis.

Surgical procedure
For patients who underwent 3D MR ECIRS, holograms were overlapped on the real anatomy to guide the surgeon during percutaneous puncture. In the standard group, the procedures were only guided by ultrasound and fluoroscopy.

Measurements
Differences in preoperative and postoperative patient characteristics between the groups were tested using a χ^2 test and a Kruskal-Wallis test for categorical and continuous variables, respectively. Results are reported as the median and interquartile range for continuous variables and as the frequency and percentage for categorical variables.

Results and limitations
Ten patients underwent 3D MR ECIRS. In all cases, the inferior calyx was punctured correctly, as planned using the overlapping hologram. The median puncture and radiation exposure times were 27 min and 120 s, respectively. No intraoperative or major postoperative complications occurred. Matched pair analysis with the standard ECIRS group revealed a significantly shorter radiation exposure time for the 3D MR group ($p < 0.001$) even though the puncture time was longer in comparison to the standard group ($p < 0.001$). Finally, use of 3D MR led to a higher success rate for renal puncture at the first attempt (100% vs 50%; $p = 0.032$). The main limitations of the study are the small sample size and manual overlapping of the rigid hologram models.

Conclusions
Our experience demonstrates that 3D MR guidance for renal puncture is feasible and safe. The procedure proved to be effective, with the inferior calyx correctly punctured in all cases, and was associated with a low intraoperative radiation exposure time because of the MR guidance.

Patient summary
Three-dimensional virtual models visualized as holograms and intraoperatively overlapped on the patient's real anatomy seem to be a valid new tool for guiding puncture of the kidney through the skin for minimally invasive treatment.

Keywords:
Three-dimensional reconstruction; Mixed realityHyper Accuracy 3D; Image-guided surgery; Kidney stones; Holograms.

1. Introduction

For kidney stones larger than 2 cm, the first-line treatment is percutaneous nephrolithotomy (PCNL) [1]. Recent technical and technological innovations have led to the development of an even more minimally invasive approach to percutaneous kidney surgery [2], [3], [4]. One of the crucial steps in this procedure is correct access to the collecting system, which is probably the most challenging maneuver, characterized by the steepest learning curve. The safety and effectiveness (stone removal) of the surgery is strictly dependent on the renal puncture. In order to prevent severe complications, excellent knowledge of the anatomy of the excretory system is required [5]. Calyceal puncture can usually be guided by ultrasound, fluoroscopy, or a combination of both [6]. These images can be suboptimal in defining complex structures, such as the renal collecting system, and its relationships with vessels and neighboring organs; therefore, many different navigation methods have been developed in recent years [7]. Among the different technologies proposed, the use of three-dimensional (3D) models obtained from preoperative computer tomography (CT) images and intraoperatively superimposed onto the in vivo anatomy seems to be one of the most promising strategies [8]. Building on these results, to enhance the surgeon's perception of the three-dimensionality of anatomical structures we developed 3D holograms of the kidney anatomy that can be overlapped onto the real environment using dedicated visors, such as the Hololens, in a mixed reality (MR) setting [9]. Here we describe a novel technique involving the use of 3D holograms and MR technology to establish access during percutaneous kidney surgery and report our first preliminary results.

2. Patients and methods

2.1. Objectives

The primary aim was to describe our new technique that uses 3D holograms and MR technology to establish a needle access point, to drive the needle route during percutaneous kidney puncture, and to report our first preliminary results. The secondary aim was to compare this novel approach (3D MR group) with the standard percutaneous puncture technique using fluoroscopy and ultrasound guidance (standard group).

2.2. Study population

This was a prospective study enrolling consecutive patients with kidney stones scheduled for endoscopic combined intrarenal surgery (ECIRS) at our center from July 2019 to January 2020. The inclusion criterion for ECIRS at our center was kidney stones (calyceal or pelvic) larger than 2 cm. Contraindications to this surgery were a history of upper urinary tract urothelial cancer, coagulation disorders, and children. The only exclusion criterion was the absence of consent to share patient data. The study was conducted in accordance with good clinical practice guidelines, and informed consent was obtained from the patients in accordance with Italian law (Agenzia Italiana del Farmaco guidelines for observational studies, March 20, 2008).

2.3. Imaging acquisition protocol and 3D model reconstruction

First, a 3-mm contrast-enhanced CT scan with basal, angiographic, nephrographic, and late phases was performed as previously described to obtain high-quality images [10]. CT image acquisition was performed with the patient in the procedural position and a short period of apnea to avoid the impact of respiratory movements on the kidney position.

Using software authorized for medical use, CT images in DICOM format were processed by Medics (Turin, Italy; www.medics3d.com). The four-phase CT images were first evaluated by a bioengineer using a DICOM viewer and the segmentation process was performed semi-automatically. The three-dimensional reconstruction obtained was then refined by a biomedical engineer under the supervision of an experienced urologist, focusing on the renal vasculature (both arterial and

venous), urinary collecting system, kidney shape, and kidney stone features. At the end of the process, a hyperaccuracy 3D (HA3D) model was created (Fig. 1) [10]. Furthermore, neighboring organs such as the spleen, liver, and colon were also segmented and three-dimensionally reconstructed.

2.4. Holograms and MR set-up

The final output was exported in .stl format and the files were subsequently converted into .obj and .mtl formats using the open-source Blender v2.79 software (Blender Foundation, Amsterdam, The Netherlands; www.blender.org/). The files, including the detailed 3D models, were then sent to Fifthingenium (Milan, Italy; https://fifthingenium.com/). These files were arranged in groups using a descriptor containing all the information for a single anatomic element (3D model), including its size, scale, color, and rotation matrix. The descriptor files for the 3D models were uploaded to a secure server running Windows Server 2016, which generates a QR code compatible with Hololens visors. All the files could subsequently be downloaded to a local hard drive.

After downloading the files, the user can select both the preloaded hologram of the 3D model and an area in its real visual environment to position it and load selected elements. At this point the MR experiment started (Fig. 2). The surgeon wearing the Hololens, while visualizing the holograms, can remove or decolor the renal parenchyma, renal pelvis, calyces, arteries, and veins using a dedicated menu. It is also possible to move and rotate the 3D hologram to gain a better understanding of the relationships between the different anatomical structures.

2.5. 3D MR percutaneous puncture

The patient was placed in the Galdakao-modified Valdivia position to better expose the flank for kidney puncture. The 3D models could then be tested again in the MR environment. The engineer helped the surgeon in the preliminary steps of overlapping the virtual model by rotating and translating it over the patient's anatomy. This was possible thanks to specific gestures that allow interaction with a bounding box around the hologram. The models were not only overlapped on the patient's anatomy but were also projected and anchored inside the patient's body thanks to the ability of the visor to distinguish different surface patterns in the environment (Fig. 3).

Using a Hololens, further refinement of the overlapping process was performed by the first surgeon. The landmarks used to drive the manual overlapping were the operative bed (longitudinal axis), a line between the iliac crest and the XIIth rib (sagittal axis), and the pubis (coronal axis; Fig. 4). Once the overlapping was considered to be correct, the surgeon could fix and block the virtual model to avoid further displacements.

After the virtual environment was set up, percutaneous puncture could be performed. A Chiba needle was put on the patient's flank while simulating its route and its entry into the inferior calyx. The correct position of the needle with respect to the calyx was checked via fluoroscopy and ultrasound, as in a standard procedure. Then percutaneous puncture was performed. Thanks to the 3D MR holograms, the surgeon had a real-time perception of the needle route and avoided the risk of damage to neighboring organs. The inferior calyx could be punctured at the papilla (Fig. 5). The kidney stones were then treated by following the standard ECIRS technique [11]. The whole 3D MR ECIRS technique is explained in the accompanying video. At the end of the procedure, fluoroscopy showed the nephrostomy correctly placed in the inferior calyx, as planned using the 3D model (Fig. 6).

2.6. 3D MR needle route evaluation

An appropriate needle route was evaluated during preoperative planning using CT images to avoid injury to adjacent anatomical structures. According to the hypothesis of Akand et al [7], the access point, direction angle, and access angle towards the stone during PCNL were calculated using CT scan data and a specific mathematical formula, namely the cosine rule. In particular, the surgeon estimated the access point identified on the CT slice and turned according to the access angle

(assumed to be 45° as described by Akand et al [7]. Then this new point has to be repositioned on the skin surface using the cosine formula to obtain the real access point [7]. The simulated needle route was subsequently reproduced in the 3D model so that the surgeon could visualize it intraoperatively using the Hololens during the puncture phase. Finally, after kidney puncture the real angle was measured using fluoroscopy images and compared with the 3D MR simulated angle (Fig. 7).

2.7. Control group

In a matched pair analysis, the patients in the 3D MR group were compared to patients in the San Luigi Hospital database (Orbassano, Turin, Italy) who underwent standard ECIRS with a combined technique (ultrasound and fluoroscopy) from 2015 performed by the same surgical team [11] with the same inclusion and exclusion criteria and the same technique [11].
To optimize the nature of the comparison with the control group (no 3D MR), we used 1:1 propensity score (PS) matching according to the nearest neighbor [12] with a caliper of 0.2.
The *PSMATCH* procedure in SAS was used. The 1:1 PS-matched cohorts (3D MR group vs control group) were balanced according to age, sex, stone volume, body mass index (BMI), stone density, and stone location (Table 1). Again, the cosine theorem was applied to bidimensional CT images to estimate the access point [13] and the same process previously described was used to evaluate the correspondence between the simulated and real puncture angle in the control group.

2.8. Data analysis

The data collected included preoperative variables such as age, sex, BMI, preoperative serum creatinine, and stone size, density, and location. Intraoperatively, we evaluated the operative, puncture, and stone treatment times; other data, such as radiation exposure time and number of attempts needed for a successful puncture, were also collected. Each attempt was defined as when the surgeon extracted the needle and performed a new puncture. The puncture time conventionally started when the surgeon wielded the needle and finished when the needle was securely in the calyceal system. The preoperatively planned puncture angle and the effective intraoperative angles were collected. In particular, the puncture angle (on the CT scan and 3D model) was measured between the planned needle route (through the previously calculated access point and the inferior calyx) and the coronal plane tangential to the skin surface. Intraoperatively, using bidimensional fluoroscopic images, the needle route was clearly visible as a radio-opaque projection, while the intercept was tangential to the skin surface.
Intraoperative and postoperative complications were recorded and classified according to the Clavien-Dindo system [14]. After the intervention, the hospital stay, catheterization time, and time to removal of the nephrostomy and double J stent were registered. At 3-mo follow-up, serum creatinine levels were measured. The success rate, defined as stone-free rate (SFR) plus the absence of clinically significant residual fragments ≤4 mm (CIRF), was analyzed.
All surgeries were performed by two experienced surgeons with more than 10 yr of experience and a personal case series of more than 200 kidney punctures each (F.P., M.C.).

2.9. Statistical analysis

Descriptive results are reported as the median and interquartile range for continuous variables and as the frequency and percentage for categorical variables.
Given the non-normal distribution for age, BMI, creatinine, stone density, operative time, puncture time, stone treatment time, and radiation exposure time, differences between the groups were evaluated using the nonparametric Kruskal-Wallis method. Median differences and their 95% confidence interval (CI) were calculated using *PROC QUANTREG* in SAS. In particular, we used the method proposed by Altman et al [15] and Hill [16] for calculations. The median difference was estimated as the median value of all possible differences between the values for the two groups. For the 95% CI we used the formula:

$$K = \frac{n_1 * n_2}{2} - \left(z_{0.95} * \sqrt{n_1 * n_2 * \frac{n_1 + n_2 + 1}{12}} \right)$$

where n_i is the size of the *i*th group. The smallest and the largest *K* values for the difference are the 95% CI.

Differences between the groups were evaluated using the χ^2 test for American Society of Anesthesiologists score, stone position, postoperative complications, and the success rate, Fisher's exact test for successful puncture at the first attempt, and the Mann-Whitney test for hospital stay, times to catheter removal, nephrostomy removal, and stent removal, and creatinine levels.

To evaluate the concordance between the planned and intraoperative puncture angles, the Bland-Altman method for agreement between quantitative measurements was applied. A mismatch of <4% was considered acceptable and was classified as good concordance [17]. All *p* values reported were obtained using the two-sided exact method at the conventional 5% significance level. Data were analyzed using SAS statistical software.

3. Results

3.1. 3D Mr Ecirs findings

Ten patients underwent 3D MR ECIRS (Table 1). The median stone size was 34.5 mm (Supplementary Table 1). In all cases, the inferior calyx was punctured correctly, as driven by the overlapping hologram.

The preoperative planned puncture angle showed optimal concordance with the 3D MR-guided intraoperative angle in all cases (mismatch <4% in 10/10 patients). The median operative time was 108 min. The median puncture time was 27 min, the median stone treatment time was 78 min, and the median radiation exposure time was 120 s (Table 2). No intraoperative or major postoperative complications occurred.

The median hospital stay was 4 d and the nephrostomy and double-J stent were removed at a median of 2 and 15 d after surgery, respectively. At 3-mo follow-up, CT imaging showed a success rate (SFR + absence of CIRF) of 100% (Table 3).

3.2. Matched pair analysis

For retrospective matched pair analysis, ten patients with same preoperative characteristics who underwent standard ECIRS were selected as the control group (Supplementary Table 2). The median radiation exposure time was significantly shorter for the 3D MR group (120 min) compared to the control group (262 min; differences in medians 138 min, 95% CI 70–205 [15], $p < 0.001$). The median puncture time was longer for the 3D MR group (27 min) compared to the control group (15 min; differences in medians 12 min, 95% CI 6–17 [15], $p < 0.001$; Table 2). Finally, use of 3D MR allowed higher concordance between the preoperative and intraoperative puncture angles in comparison to the control group (100% vs 50%; $p = 0.009$); moreover, the rate of successful first attempts at renal puncture was greater for the 3D MR group (100% vs 50%; $p = 0.032$).

4. Discussion

The present study shows the feasibility of 3D MR-guided percutaneous puncture for the first time and confirms the accuracy of 3D model reconstructions and of the manual overlapping process. The ability to visualize MR images three-dimensionally in real-time allowed us to correctly reproduce the planned puncture needle route intraoperatively in all cases (100% vs 50% in the control group; $p = 0.032$).

Our findings push towards the development of precision surgery: for each patient, a unique 3D model was created and subsequently visualized as a hologram. This technology was used for both surgical planning and intraoperative navigation. In the percutaneous approach to renal stones, renal puncture is probably the most difficult step. Precise identification of the puncture site is mandatory for performing a correct procedure. Fluoroscopy, ultrasound, or a combination of the two are the imaging techniques most commonly used, with fluoroscopy being the gold standard. However, in patients with congenital (eg, horseshoe kidney) or acquired (eg, renal cysts, history of urological surgery) anatomical anomalies, puncture can be difficult, making supplementary imaging necessary in order to perform a safe procedure. For this reason, preoperative contrast-enhanced CT with a urographic phase is now strongly recommended for every case of complicated nephrolithiasis [1]. To further improve the aforementioned imaging techniques, 3D models can be created [10], [18] and displayed three-dimensionally as holograms [9].
However, as these imaging techniques are unsuitable for building an intraoperative navigation system, the needle route remains undetermined, with a consequent potential risk of damaging nearby structures. Mozer et al [19] were the first to describe a computer-assisted guidance system that allowed projection of ultrasound images over preoperative fluoroscopic images. Their results are still preliminary since they were obtained from one phantom and one patient. Encouraging results were reported by Oliveira-Santos et al [20], who published a study describing a stereotactic needle guidance system for PCNL on prototype phantoms. After the development process for new technologies started to involve the world of robotics, the PAKY-RCM (percutaneous access to the kidney remote center of motion) device was created [21]. This robotic arm provided similar results compared to manual puncture and reduced the overall fluoroscopy time, with minor operator radiation exposure. In 87% (20/23) of the cases the puncture was successful, while in the remaining cases the surgeon had to switch to conventional techniques. The main disadvantage of this new technology is its high cost [21]. Electromagnetic tracking (EMT) allows localization of a sensor placed at the tip of a ureteral catheter, up to the calyceal system. Rodrigues et al [22] slightly modified this procedure by attaching the sensor to the tip of a ureteroscope and placing the sensor directly in the selected calyx. EMT allows real-time tracking, but cannot provide satisfactory visualization of the surrounding anatomical structures [22]. Several alternative techniques have been tried, such as the AcuBot robot (an intraoperative CT-guided system) [23] and Syngo-iGuide (a laser technology-based software) [24]. However, these are complex and expensive solutions that do not find real application in daily practice. To perform a precise puncture during PCNL, Akand et al [7] described an innovative technique that involves the use of dedicated mathematical software, 3D modeling, and augmented reality. First results obtained from two procedures on ex vivo models are promising. Another recently described innovation is the iPad-assisted technique created by Müller et al [25] for performing percutaneous puncture and used in a phantom study. After embedding porcine kidneys in ballistic gelatin, the authors punctured the calyceal system using an iPad, ultrasound, and fluoroscopy guidance. This technique showed optimal results, with lower fluoroscopy and access times for both novice and expert urologists. Rassweiler-Seyfried et al [26] were the first to test the iPad-assisted navigation system in an actual operating room, but no significant differences in the number of puncture attempts were found when the technique was compared to standard methods. However, longer radiation exposure and puncture times were recorded. Kratiras et al [27] have tested a tablet-based image-guided surgical system in a different urological setting.
Our experiment fits perfectly in this context. Using a patient-specific hologram intraoperatively overlapped on the patient's body, the entire percutaneous puncture process can be driven by virtual images. To the best of our knowledge, this is the first time that holograms were used intraoperatively in real time to guide the surgeon during a specific step of the procedure. The interaction between virtual images and the real environment represents a milestone in the image-guided surgery era [28]. In this context, the term "mixed reality" refers to the mix of the user's real world and the digitally created models, which can interact and coexist. In our experience, percutaneous puncture performed under MR guidance seems to be feasible and safe. In terms of

intraoperative variables, 3D MR was associated with a higher rate of first-attempt successful punctures compared to the control group (100% vs 50%; $p = 0.032$). This result suggests that the technology could have a potential role in the learning curve of inexperienced surgeons. Postoperative variables (even in terms of complications) were similar between the two groups, probably because of the small sample size and the surgeons' high experience.

The innovative technology and technique presented here are not devoid of limitations. In terms of imaging, a four-phase CT scan is necessary to obtain HA3D images and therefore the goal of the ALARA principles was not reached [29]. In addition, this technology (HA3D models) is not available in the majority of centers and requires a close-knit team of surgeons and biomedical engineers for a time-consuming process that requires segmentation not only of the kidney and stone but also of the liver, spleen, and spinal column.

Second, the overlapping process is still manual and requires anatomical landmarks such as the pubis, ribs, and iliac crests. Further research is needed to develop software for fully automatic overlapping. Third, the display of the virtual anatomy over the patient's real anatomy is still unsatisfactory, with respiratory movements and organ deformation the main issues to be solved. Artificial intelligence in this setting may play a crucial role [30]. Furthermore, the data are from a single high-volume referral center and might not be comparable to other settings, especially in terms of complications. Moreover, all the procedures were performed by expert surgeons with extensive experience in percutaneous puncture. Lastly, the retrospective matched nature of our study affects the comparative outcomes.

This technology is still in an embryonic phase: with 3D MR percutaneous puncture attracting increasing interest, potential future application, especially in complex cases with peculiar anatomical conditions, will be possible. Looking to the future, the natural evolution of this technology will be totally automatic overlapping. In particular, two approaches could be suitable: the first involves the use of external markers (such as QR codes or IR tabs) applied at the level of the operative table, iliac spine, or ribs to anchor the 3D images; the second is based on the ability of the "virtual eyes" of the surgeon (the head-mounted display system) to recognize the patient's position and automatically overlap the models via deep-learning artificial intelligence algorithms.

5. Conclusions

Our pioneering experience demonstrates that renal puncture guided by 3D mixed reality is an effective procedure thanks to the real-time needle route guidance. Moreover, it seems to be successful and safe, with the inferior calyx correctly punctured in all cases, and with a low intraoperative radiation exposure time thanks to MR guidance but with an increased total radiation exposure due to preoperative four phase CT scan. Further research is necessary to support these promising results, as the current evidence remains limited.

Author contributions: Enrico Checcucci had full access to all the data in the study and takes responsibility for the integrity of the data and the accuracy of the data analysis.
Study concept and design: Porpiglia.
Acquisition of data: Niculescu, Peretti, De Cillis, Piana, Piramide.
Analysis and interpretation of data: Piramide, Verri.
Drafting of the manuscript: Checcucci, Amparore, Porpiglia.
Critical revision of the manuscript for important intellectual content: Fiori, Manfredi, Poggio.
Statistical analysis: Stura, Migliaretti.
Obtaining funding: None.
Administrative, technical, or material support: None.
Supervision: Porpiglia, Cossu.
Other: None.

Financial disclosures*:* Enrico Checcucci certifies that all conflicts of interest, including specific financial interests and relationships and affiliations relevant to the subject matter or materials discussed in the manuscript (eg, employment/affiliation, grants or funding, consultancies, honoraria, stock ownership or options, expert testimony, royalties, or patents filed, received, or pending), are the following: None.

Funding/Support and role of the sponsor: None.

Acknowledgments: We would like to thank Dr. Andrea Bellin and Dr. Diego Manfrin for their assistance with this study.

References

[1] Türk C, Petrˇík A, Sarica K, et al. EAU guidelines on interventional treatment for urolithiasis. Eur Urol 2016;69:475–82. https://doi. org/10.1016/j.eururo.2015.07.041.
[2] Stern KL, Sivalingam S. Retrograde intrarenal surgery versus percutaneous surgery: do we have a winner? Minerva Urol Nefrol 2018;70:4–5. https://doi.org/10.23736/S0393-2249.17.03036-3.
[3] Zhang B, Xie H, Hu Y, Liu C. The visual percutaneous nephrolithotomy versus the conventional percutaneous nephrolithotomy in treatment for renal stone. Minerva Urol Nefrol 2019;71:627–35. https://doi. org/10.23736/S0393-2249.19.03465-9.
[4] Porpiglia F, Cossu M, Poggio M, et al. 701 Endoscopic combined intra renal surgery (ECIRS): 10 years of experience. Eur Urol Suppl 2015;14:. https://doi.org/10.1016/S1569-9056(15)60693-5e701.
[5] de la Rosette JJMCH, Opondo D, Daels FPJ, et al. Categorisation of complications and validation of the Clavien score for percutaneous nephrolithotomy. Eur Urol 2012;62:246–55. https://doi.org/ 10.1016/j.eururo.2012.03.055.
[6] Rodrigues PL, Rodrigues NF, Fonseca J, Lima E, Vilaca JL. Kidney targeting and puncturing during percutaneous nephrolithotomy: recent advances and future perspectives. J Endourol 2013;27: 826–34. https://doi.org/10.1089/end.2012.0740.
[7] Akand M, Civcik L, Buyukaslan A, et al. Feasibility of a novel technique using 3-dimensional modeling and augmented reality for access during percutaneous nephrolithotomy in two different exvivo models. Int Urol Nephrol 2019;51:17–25. https://doi.org/ 10.1007/s11255-018-2037-0.
[8] Detmer FJ, Hettig J, Schindele D, Schostak M, Hansen C. Virtual and augmented reality systems for renal interventions: a systematic review. IEEE Rev Biomed Eng 2017;10:78–94. https://doi.org/ 10.1109/RBME.2017.2749527.
[9] Checcucci E, Amparore D, Pecoraro A, et al. 3D mixed reality holograms for preoperative surgical planning of nephron-sparing surgery: evaluation of surgeons' perception. Minerva Urol Nefrol 2021;73:367–75. https://doi.org/10.23736/S2724-6051.19.03610-5.
[10] Porpiglia F, Bertolo R, Checcucci E, et al. Development and validation of 3D printed virtual models for robot-assisted radical prostatectomy and partial nephrectomy: urologists' and patients' perception. World J Urol 2018;36:201–7. https://doi.org/10.1007/ s00345-017-2126-1.
[11] Scoffone CM, Cracco CM, Cossu M, Grande S, Poggio M, Scarpa RM. Endoscopic combined intrarenal surgery in Galdakao-modified supine Valdivia position: a new standard for percutaneous nephrolithotomy? Eur Urol 2008;54:1393–403. https://doi.org/ 10.1016/j.eururo.2008.07.073.
[12] Austin PC. An introduction to propensity score methods for reducing the effects of confounding in observational studies. Multivariate Behav Res 2011;46:399–424. https://doi.org/10.1080/00273171. 2011.568786.
[13] Akand M, Buyukaslan A, Servi S, Civcik L. A hypothetical method for calculation of the access point, direction angle and access angle for percutaneous nephrolithotomy. Med Hypotheses 2019;124:101–4. https://doi.org/10.1016/j.mehy.2019.02.007.
[14] Dindo D, Demartines N, Clavien PA. Classification of surgical complications: a new proposal with evaluation in a cohort of 6336 patients and results of a survey. Ann Surg 2004;240:205–13. https://doi.org/10.1097/01.sla.0000133083.54934.
[15] Altman DG, Machin D, Bryant TN, Gardner MJ. Statistica medica. Intervalli di confidenza nella ricerca biomedica. Turin, Italy: Edizioni Minerva Medica; 2004.
[16] Hill ID. C281. 95% confidence limits for the median. J Stat Comput Simul 1987;28:80–1. https://doi.org/10.1080/00949658708811012.
[17] Weinfurt PT. Biomedical technology assessment: the. 3Q method. ed. 1. San Rafael, CA: Morgan and Claypool Publishers; 2010. p. 16–8.
[18] Li H, Chen Y, Liu C, Li B, Xu K, Bao S. Construction of a threedimensional model of renal stones: comprehensive planning for percutaneous nephrolithotomy and assistance in surgery. World J Urol 2013;31:1587–92. https://doi.org/10.1007/s00345-012-0998- 7.

[19] Mozer P, Conort P, Leroy A, et al. Aid to percutaneous renal access by virtual projection of the ultrasound puncture tract onto fluoroscopic images. J Endourol 2007;21:460–5. https://doi.org/ 10.1089/end.2006.0168.
[20] Oliveira-Santos T, Peterhans M, Roth B, et al. Computer aided surgery for percutaneous nephrolithotomy: clinical requirement analysis and system design. In: Proceedings of the 2010 Annual International Conference of the IEEE Engineering in Medicine and Biology Society. New York, NY: IEEE; 2010. p. 442–5. https://doi. org/10.1109/IEMBS.2010.5627387.
[21] Su LM, Stoianovici D, Jarrett TW, et al. Robotic percutaneous access to the kidney: comparison with standard manual access. J Endourol 2002;16:471–5. https://doi.org/10.1089/089277902760367421.
[22] Rodrigues PL, Vilaca JL, Oliveira C, et al. Collecting system percutaneous access using real-time tracking sensors: first pig model in vivo experience. J Urol 2013;190:1932–7. https://doi.org/ 10.1016/j.juro.2013.05.042.
[23] Pollock R, Mozer P, Guzzo TJ, et al. Prospects in percutaneous ablative targeting: comparison of a computer-assisted navigation system and the AcuBot robotic system. J Endourol 2010;24: 1269–72. https://doi.org/10.1089/end.2009.0482.
[24] Ritter M, Rassweiler MC, Hacker A, Michel MS. Laser-guided percutaneous kidney access with the Uro Dyna-CT: first experience of three-dimensional puncture planning with an ex vivo model. World J Urol 2013;31:1147–51. https://doi.org/ 10.1007/s00345-012-0847-8.
[25] Müller M, Rassweiler M-C, Klein J, et al. Mobile augmented reality for computer-assisted percutaneous nephrolithotomy. Int J Comput Assist Radiol Surg 2013;8:663–75. https://doi.org/10.1007/s11548- 013-0828-4.
[26] Rassweiler-Seyfried MC, Rassweiler JJ, Weiss C, et al. iPad-assisted percutaneous nephrolithotomy (PCNL): a matched pair analysis compared to standard PCNL. World J Urol 2020;38:447–53. https:// doi.org/10.1007/s00345-019-02801-y.
[27] Kratiras Z, Gavazzi A, Belba A, et al. Phase I study of a new tabletbased image guided surgical system in robot-assisted radical prostatectomy. Minerva Urol Nefrol 2019;71:92–5.
[28] Veneziano D, Amparore D, Cacciamani G, et al. Climbing over the barriers of current imaging technology in urology. Eur Urol 2020;77:142–3. https://doi.org/10.1016/j.eururo.2019.09.016.
[29] Chen TT, Preminger GM, Lipkin ME. Minimizing radiation exposure during percutaneous nephrolithotomy. Minerva Urol Nefrol 2015;67:347–54.
[30] Checcucci E, Autorino R, Cacciamani GE, et al. Artificial intelligence and neural networks in urology: current clinical applications. Minerva Urol Nefrol 2020;72:49–57. https://doi.org/10.23736/ S0393-2249.19.03613-0.

Table 1. Preoperative patient characteristics

Parameter	3D MR group	Standard group	*p* value
Median age, yr (IQR)	56.0 (54.0–57.0)	56.0 (54.0–58.0)	0.9
Male, *n* (%)	6 (60)	5 (50)	0.6
Median body mass index, kg/m^2 (IQR)	26.0 (25.0–27.0)	27.0 (26.0–28.0)	0.1
ASA score, *n* (%)			1
ASA 1	1 (10)	1 (10)	
ASA 2	8 (80)	8 (80)	
ASA 3	1 (10)	1 (10)	
ASA 4	0 (0)	0 (0)	
Median preoperative creatinine, mg/dl (IQR)	1.0 (0.9–1.2)	1.0 (0.9–1.4)	0.6
Median stone size, mm (IQR)	34.5 (33.0–35.0)	37.0 (35.0–38.0)	0.5
Median stone density, HU (IQR)	986.0 (975.0–988.0)	1076.0 (1043.0–1089.0)	0.1
Stone position, *n* (%)			0.8
Upper calyx	1 (10)	1 (10)	
Middle calyx	2 (20)	3 (30)	
Inferior calyx	3 (30)	1 (10)	
Renal pelvis	2 (20)	2 (20)	
Partial staghorn stones	2 (20)	3 (30)	

3D = three-dimensional; ASA = American Society of Anesthesiologists; HU = Hounsfield units; IQR = interquartile range; MR = mixed reality.

Table 2. Intraoperative variables

	3D MR group	Standard group	MD (95% CI)	p value
Median operative time, min (IQR)	108.0 (105.0–124.0)	91.0 (90.0–95.0)	15.0 (3.5–26.4)	0.020
Median puncture time, min (IQR)	27.0 (24.0–28.0)	15.0 (11.0–18.0)	12.0 (6.8–17.1)	<0.01
Median stone treatment time, min (IQR)	78.0 (76.0–80.0)	76.5 (74.0–78.0)	−1.0 (−4.9 to 2.9)	0.2
Median radiation exposure time, s (IQR)	120.0 (100.0–127.0)	262.0 (256.0–289.0)	−138.0 (−205.3 to −70.6)	<0.01
Intraoperative complications, n (%)	0 (0)	0 (0)		–
First attempt at renal puncture successful, n (%)	10/10 (100)	5/10 (50)		0.032

3D = three-dimensional; CI = confidence interval; IQR = interquartile range; MD = median difference; MR = mixed reality.

Table 3. Perioperative and postoperative data

	3D MR group	Standard group	MD (95% CI)	p value
Median hospital stay, d (IQR) [a]	4.0 (4.0–5.0)	4.0 (3.0–4.0)	0 (−0.7 to 0.7)	0.058
Median time to vesical catheter removal, d (IQR) [a]	1.0 (1.0–1.0)	1.0 (1.0–2.0)	0 (−0.7 to 0.7)	0.6
Median time to nephrostomy removal, d (IQR) [a]	2.0 (2.0–2.0)	2.0 (2.0–2.0)	0	1
Median time to double-J stent removal, d (IQR) [a]	15.0 (14.0–17.0)	15.5 (14.0–16.0)	0 (−2.3 to 2.3)	0.5
Median creatinine at discharge, mg/dl (IQR)	1.0 (0.6–1.2)	1.0 (0.9–1.2)	0 (−0.3 to 0.3)	0.7
Postoperative complications, n (%)				0.4
Clavien ≤2	3 (30)	3 (30)		
Hematuria	2 (20)	2 (20)		
Fever	1 (10)	0 (0)		
Urinary retention	0 (0)	1 (10)		
Clavien ≥3	0 (0)	1 (10)		
Ureteral stenosis	0 (0)	1 (10)		
Median creatinine at 3 mo, mg/dl (IQR)	1.0 (0.6–1.1)	1.0 (0.9–1.1)	0 (−0.3 to 0.3)	0.5
Success at 3 mo, n (%) [b]	10/10 (100)	9/10 (90)		0.3

3D = three-dimensional; CI = confidence interval; IQR = interquartile range; MD = median difference; MR = mixed reality.

[a]Time from first postoperative day.

[b]Success defined as completely stone-free or clinically insignificant residual fragment ≤4 mm at 3-mo computed tomography scan.

Fig. 1. Hyper Accuracy 3D reconstruction of the kidney, vessels, calyx, and stone.

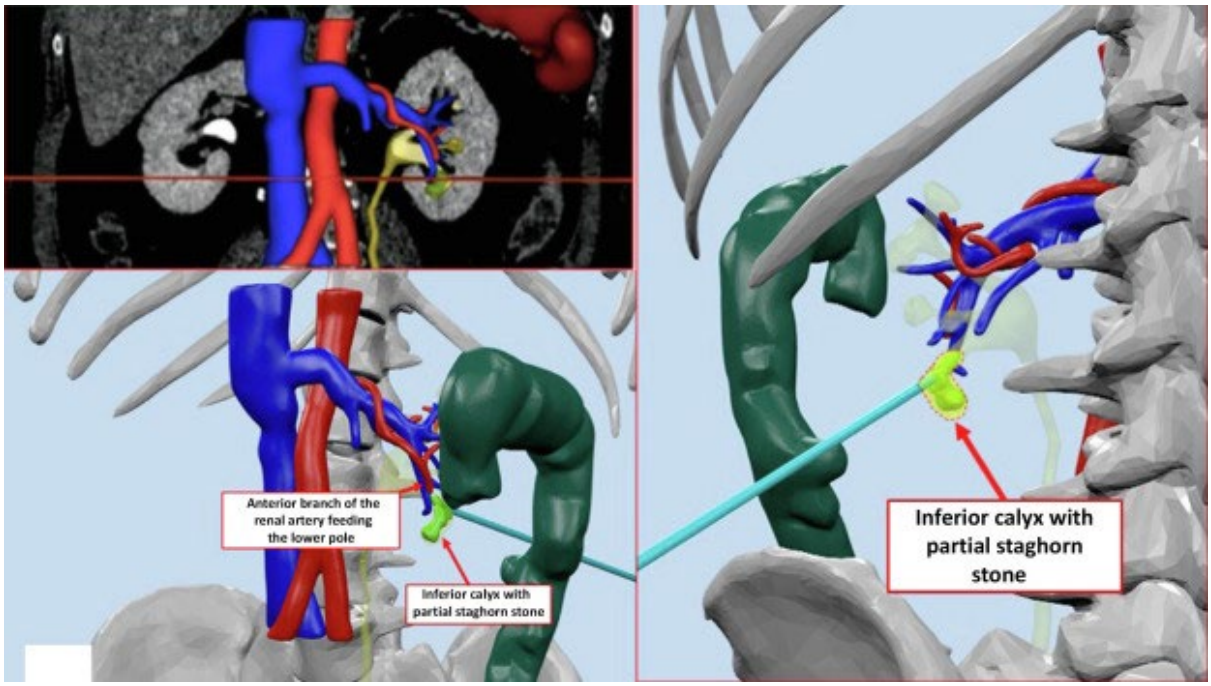

Fig. 2. Hyper Accuracy 3D model visualized as a hologram.

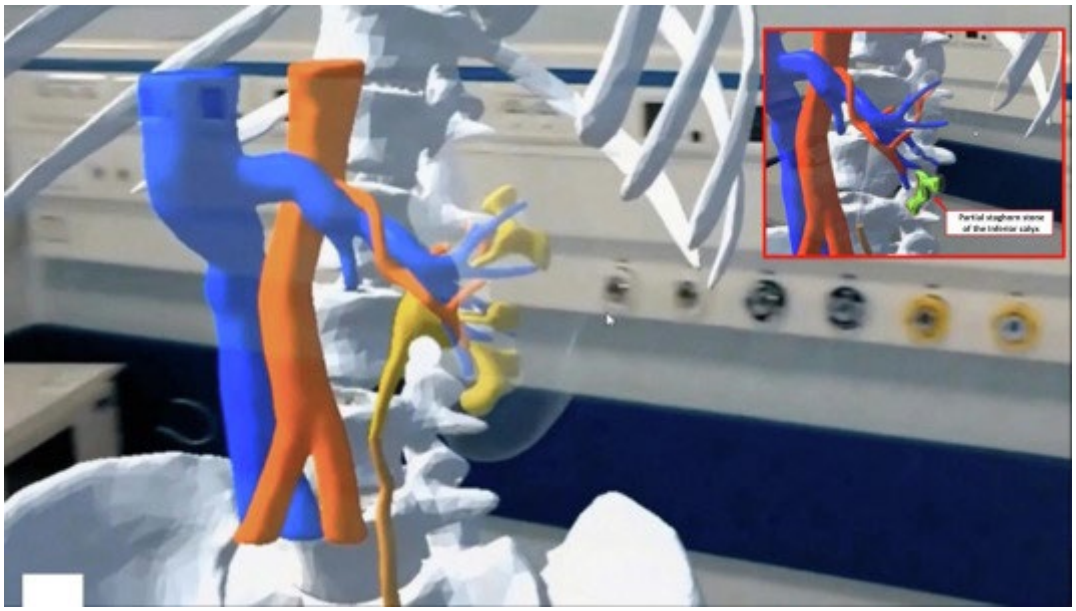

Fig. 3. The three-dimensional hologram was overlapped inside the patient's anatomy using a Hololens to identify different environmental surface patterns.

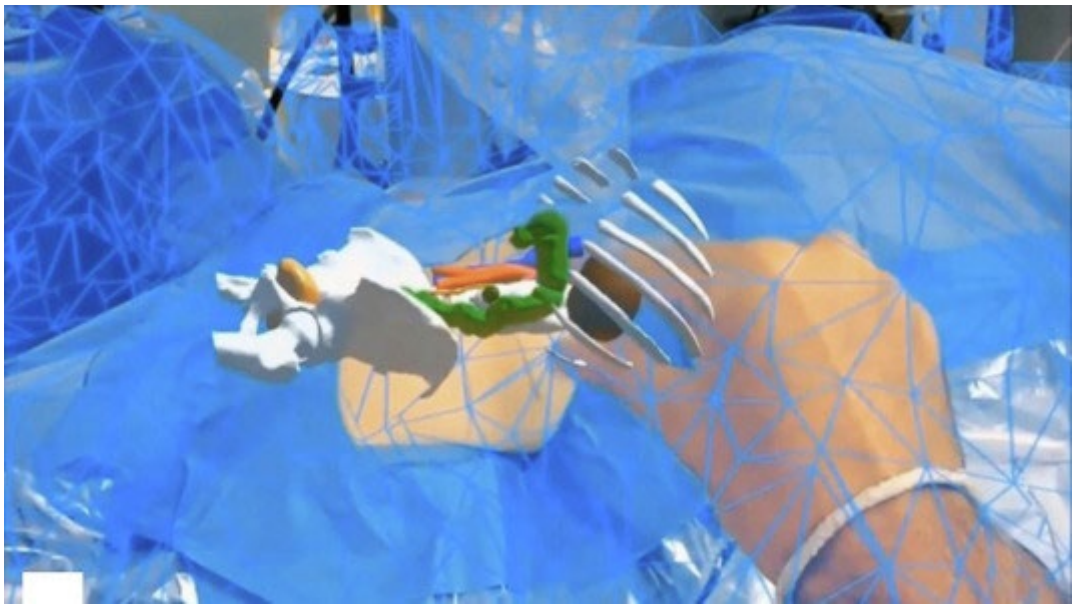

Fig. 4. The three-dimensional hologram was correctly overlapped onto the patient using visual landmarks such as the anterior iliac spine, XIIth rib, pubis, and operative table.

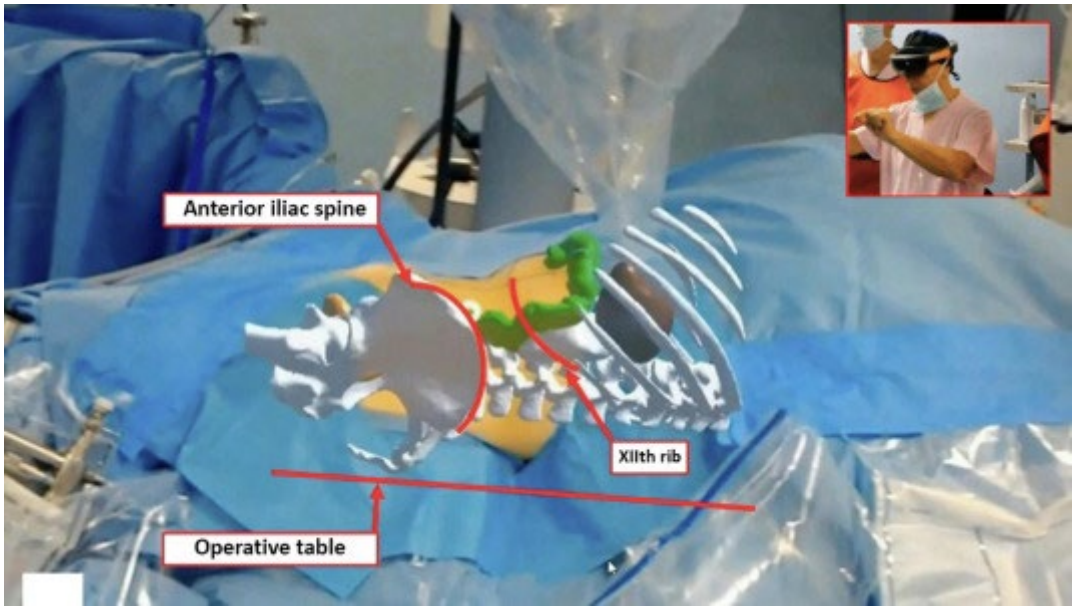

Fig. 5. Under three-dimensional hologram guidance, the inferior calyx was correctly punctured as shown by fluoroscopic and endoscopic images.

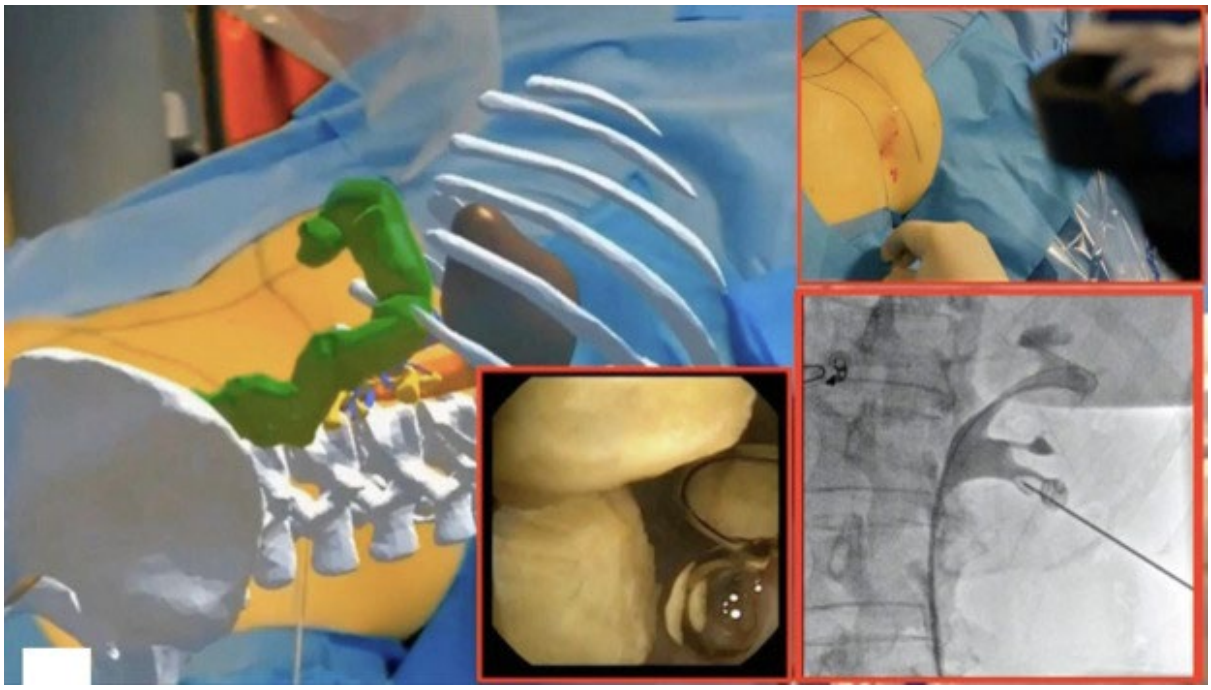

Fig. 6. At the end of the procedure, fluoroscopy showed the nephrostomy correctly placed in the inferior calyx, as planned via three-dimensional simulation.

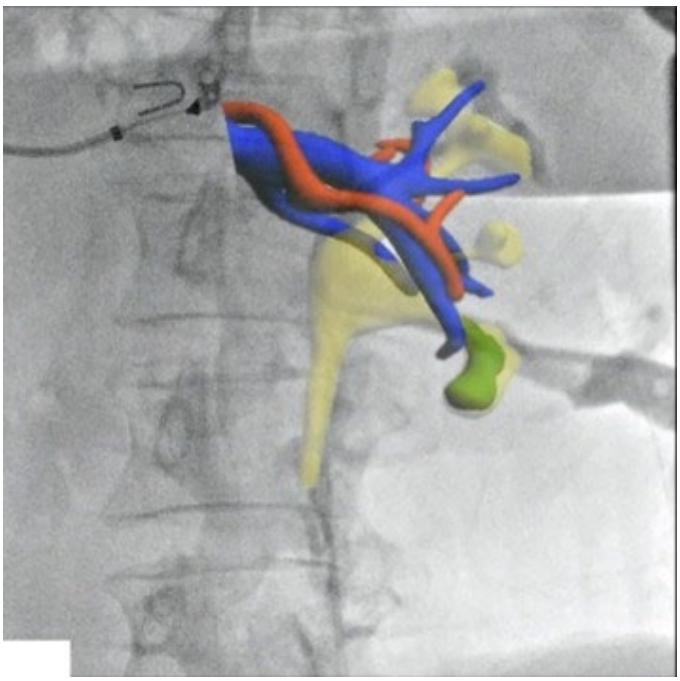

Fig. 7. The preoperatively planned puncture angle matched with the fluoroscopic one, in accordance with the three-dimensional mixed-reality guidance system. CT = computed tomography.